OFFICE OF NAVAL RESEARCH

GRANT or CONTRACT: N00014-91-J-1919

R&T Code 4133036
Robert Nowak

Technical Report No. 14

Electrochemical Epitaxy

Huang M. Baoming, Tedd E. Lister and John L. Stickney

In Press

in

"Handbook of Surface Imaging and Visualization"
CRC Press

Department of Chemistry
University of Georgia
Athens, GA 30602-2556

6/24/94

REPORT DOCUMENTATION PAGE

Form Approved
OMB No. 0704-0188

1. AGENCY USE ONLY (Leave blank)	2. REPORT DATE	3. REPORT TYPE AND DATES COVERED
	6/25/94	Technical - 1, June

4. TITLE AND SUBTITLE
Electrochemical Epitaxy

5. FUNDING NUMBERS
G-N00014-19-J-1919

6. AUTHOR(S)
Huang M. Baoming, Tedd E. Lister and John L. Stickney

7. PERFORMING ORGANIZATION NAME(S) AND ADDRESS(ES)
John L. Stickney
Department of Chemistry
University of Georgia
Athens, GA 30602-2556

8. PERFORMING ORGANIZATION REPORT NUMBER
Technical Report #14

9. SPONSORING/MONITORING AGENCY NAME(S) AND ADDRESS(ES)
Office of Naval Research
Chemistry Division
Arlington, VA 22217-5000

10. SPONSORING/MONITORING AGENCY REPORT NUMBER

11. SUPPLEMENTARY NOTES

12a. DISTRIBUTION/AVAILABILITY STATEMENT
Approved for public release and sale;
its distribution is unlimited

12b. DISTRIBUTION CODE

13. ABSTRACT (Maximum 200 words)

This chapter discusses epitaxy in electrodeposition. The paper mostly discusses compound epitaxy in electrodeposition. This can include the surface compounds formed by the UPD on one element on a second element. It also includes the formation of thin films and bulk compounds on various substrates. A discussion of electrochemical atomic layer epitaxy is included as well.

14. SUBJECT TERMS
Epitaxy, UPD, II-VI compounds, electrodeposition, ECALE

15. NUMBER OF PAGES
40

16. PRICE CODE

17. SECURITY CLASSIFICATION OF REPORT	18. SECURITY CLASSIFICATION OF THIS PAGE	19. SECURITY CLASSIFICATION OF ABSTRACT	20. LIMITATION OF ABSTRACT
Unclassified	Unclassified	Unclassified	UL

ELECTROCHEMICAL EPITAXY

Huang M. Baoming, Todd E. Lister and John L. Stickney*,

Department of Chemistry,

University of Georgia,

Athens, Georgia 30602-2556.

* To whom correspondence should be addressed.

INTRODUCTION

The present discussion will be limited, for the most part, to consideration of the epitaxial electrodeposition of compounds. Discussions of epitaxy associated with the deposition of thin films of one element on a second element can be found in several references [1-3]. The homoepitaxial electrodeposition of elements, although very interesting, is relatively more common and will not be discussed here [2].

The electrodeposition of a single atomic layer of an element on a foreign elemental substrate, represents the limit in compound formation. Frequently, the first atomic layer of the depositing element forms at a potential prior to, under, that needed to deposit the bulk element. This phenomenon is referred to as underpotential deposition (UPD). UPD is an important, well studied and reviewed area of electrochemical surface science [4-6]. In general, UPD results in deposits one atom thick (an atomic layer), although the absolute coverage is frequently some function of the deposition potential. In some cases, the deposits can be thought of as resulting in formation of a surface compound, such as when the adlattice has a well-defined relationship with the substrate surface atoms (is commensurate), and has a specific coverage. Other systems have a less well defined relationship with the substrate surface atoms, forming incommensurate adlattices, with coverages which are continuously dependent on the deposition potential. Those systems might be better classed as surface alloys.

As can be seen from the literature [4-6], a very large number of metal-metal UPD systems have been investigated. The metal-metal systems studied have nearly always involve Reductive UPD. That is, an atomic layer is formed by reduction of a species containing the element in a positive oxidation state:

{1} $Cu^{+2} + 2e^{-} \Longrightarrow Cu_{(UPD)}$,

for example, at a potential above that needed to deposit bulk Cu. In addition to the UPD of metals, a classic Reductive UPD system is the hydrogen waves on Pt. The hydrogen waves correspond to the reduction of protons at potentials above that needed to form bulk H_2 gas.

Observed reduction currents are ascribed to the formation of a monolayer of hydrogen atoms on the Pt electrode surface [7-8].

Atomic layers of a number of elements can be formed by Oxidative UPD, as well:

{2} $S^{2-} \longrightarrow S(UPD) + 2e^-$

for example, at potentials below that needed to deposit the bulk element. Most of the elements which can undergo Oxidative UPD are not transition metals but main group elements such as the halides (Cl^- [9] , Br^- [10], and I^- [11]), chalcogenides (O^{-2} [12], S^{2-} [12, 13], Se^{2-} [14], and Te^{2-} [15, 16]), and pnictides (As^{3-} [17] and Sb^{3-}).

The structures of atomic layers formed by UPD have been studied using techniques such as low energy electron diffraction (LEED) [18], scanning tunneling microscopy (STM) [16, 19-22], atomic force microscopy (AFM) [23-25] and X-ray scattering [26-30], as well as by a host of other structurally less specific techniques. In general, UPD deposits are not epitaxial in the strictest since. That is, well-ordered adlattices have been formed in a number of systems, however, the atomic layers do not exhibit unit coverage and a (1X1) unit cell. Close packed incommensurate adsorbate layers have been observed, as have commensurate adsorbate layers with specific coverages and well-defined adlattice structures. However, due to lattice mismatch problems and weak substrate adsorbate interactions, (1X1) unit cells, at unit coverage, are not generally observed.

Most UPD systems that have been well characterized involve relatively noble metals, (Pt, Au, Ag, Cu..), as opposed to the more common and reactive transition metals. The noble metals are stable in aqueous solutions and thus more readily studied. However, metals such as Au tend to have a limited surface electronic corrugation. This may account for some of the ease with which UPD adlattices adopt incommensurate structures on the surface of Au [29]. The structures of the adsorbate layers appear to be more controlled by adatom-adatom interactions, then by the substrate structure and adatom-substrate interactions.

The UPD of halides on Au [11, 29, 30-35] vs on Pt [36-39] serves as a good example of some of the kinds of behavior observed in UPD systems in general [40]. On Au(111), Oxidative UPD of I^- results in formation of an I atom adlattice. The coverage of I, however, is a continuous function of potential. That is, as the potential is increased, so is the I atom packing density [29, 30]. The I atoms show little tendency to register with the Au(111) surface in one

dimension. This is consistent with the low electronic corrugation, and that Au is an s^1 metal (that it has one electron in the non-directionally specific outer s orbital). In the case of Oxidative UPD of I^- to form I atoms on Pt, again the I atom coverage increases as the potential increases, however, instead of the continuous compression of the unit cell, observed on Au(111), the I atoms adopt a sequence of commensurate structures, each corresponding to a slightly higher I atom coverage [36-39]. That is, at more positive potentials, the driving force for packing I atoms on the surface increases until a phase transition occurs and a new commensurate structure is formed. This behavior is consistent with Pt having an unfilled d shell, and thus bonds with much more directionality than the corresponding Au surfaces [40]. As mentioned above, however, the I atoms do not form a commensurate (1X1) on either surface, as the I atoms are too large to pack tightly enough

The UPD of chalcogenides differs significantly from the frequently studied UPD of s^1 metals (Cu and Ag) and of halides, in that the chalcogenides tend to form more defined surface structures, which are generally commensurate. In addition, the adsorbate-adsorbate interactions between chalcogenide atoms are less like marbles in a box, as observed for the s^1 metals and halides. The chalcogenides frequently show unique geometries with respect to each other: dimes, chains [16] and small geometric clusters [41-43]. This type of bonding is not unexpected, given the bulk structures of the elements themselves. That is, in bulk structures of S, Se and Te, fairly strong bonds exist between adjacent atoms of the chalcogenide in a chain, but fairly weak metallic interactions exist between the atoms in different chains [44].

The formation of oxides on metal surfaces is an extreme example of the directionality exhibited by the chalcogenides in surface structures. Formation of an oxide monolayer on Au or Pt generally results in a disordered surface. The lattice parameters for the oxide control the structure of the oxide "monolayer". The oxide structure is incompatible with the metal substrate lattice constants and thus with epitaxial registry. The critical thickness in oxide formation is frequently less then a single monolayer, due to the lattice mismatch and the rigidity of the bonding [45-47]. Further down the periodic table, however, reactions forming the corresponding surface sulfides, selenides and tellurides, prove more flexible. UPD layers of selenium and tellurium on Au substrates, for instance, are well ordered at the monolayer level (Figure 1).

The electrochemical formation of epitaxial thin-films of compounds is the next topic in this discussion. Many compounds have been deposited electrochemically [48], however the importance of epitaxy has not been the focus of most previous work. For example, an extensive number of studies have been performed concerning the electrodeposition of II-VI compounds [48-50]. Over 150 papers have been published in the area, beginning as much as 30 years ago [51, 52]. A number of different electrodeposition procedures have been applied, however the majority of previous work can be characterized as using one of two basic methodologies. Most of the earliest work made use of a methodology where a metal electrode, such as Cd, was oxidized in a solution containing a chalcogenide ion, such as S^{2-} [53-60]. This procedure resulted in precipitation of a thin-film of CdS on the electrode surface. Obvious problems with the methodology are the need for migration of Cd^{+2} ions out through the films, or of S^{2-} ions into the films. The films were thus limited in thickness, were polycrystalline or amorphous, and of a generally poor quality. The second extensively used methodology involved the co-deposition of elements to form stoichiometric deposits [61, 62]. It involved the use of a solution containing precursors to both the group II and group VI elements, making up the compound. The elements were deposited simultaneously, at a constant potential, from a single solution. In a sense, UPD played an important roll in that methodology. To form CdTe, for example, a low concentration of the Te precursor, $HTeO^{+}_{2}$, was used. The solution also contained a relatively high concentration of the Cd precursor, Cd^{+2}. The potential was chosen low enough for $HTeO^{+}_{2}$ reduction to be mass transfer limited, yet high enough so that Cd UPD on the Te occurred, but no bulk Cd deposition. In principle, no bulk Te should be formed by this procedure, as when a Te atom is deposited, it reacts immediately with the ubiquitous Cd^{+2} ions. In general, however, the results of this methodology were polycrystalline deposits, as well, often with very convoluted morphologies.

The two methodologies, discussed above, do not involve mechanisms that necessarily result in the formation of epitaxial electrodeposits. The codeposition methodology appears to result in relatively better deposits than does the precipitation methodology, however. That little attention has been placed on epitaxy, can be seen in that in nearly all studies, using either methodology, the structures of the substrates were ill defined. Reports of epitaxy, in the

literature, for these systems, are nearly nonexistent [63]. The fact that the codeposition methodology involves a significant overpotential in the deposition of the chalcogen, combined with the low deposition temperatures generally used, keeps the mobilities of the depositing atoms low and thus the formation of epitaxial deposits unlikely.

Single crystalline electrodeposits of many compounds have been formed, many using electrodeposition schemes similar to the co-deposition methodology mentioned above. The growth of single crystals of compounds electrochemically indicates that homoepitaxial electrodeposition has occurred [64, 65]. The extent to which heteroepitaxial electrodeposition occurs is not as clear, however. Very little work [63], beyond studies of UPD, has been performed addressing the heteroepitaxial formation of compounds electrochemically.

Work in the author's group centers on developing methodologies for the epitaxial electrodeposition of compound semiconductors. The basis for that work is the development of an electrochemical analog to atomic layer epitaxy (ALE) [66-68], ECALE [49, 69]. ALE is a method for the formation of compounds an atomic layer at a time. A cycle is used, where atomic layers of the component elements are deposited alternately, in a cycle. One cycle results in the formation of a monolayer of the compound. ALE was developed as a chemical vapor deposition methodology (CVD), using a gas phase reactor, and the substrate temperature to control reactivity.

The principle of ECALE is the same as in ALE, to grow compounds epitaxially, an atomic layer at a time. In ECALE, however, UPD is used instead of the substrate temperature to limit the extent of an elements deposition to an atomic layer. To use UPD to deposit each element, Reductive UPD is used to deposit one of the elements, and Oxidative UPD is used to deposit the other. In the case of CdS formation [13], for example, the Cd is deposited from a solution containing Cd^{+2} by Reductive UPD (equation {1}). The solution is then exchanged for one containing S^{2-}, or HS^{-}, and Oxidative UPD of S is performed (equation {2}). These steps constitute an ECALE cycle, and thin films are formed by repeating the cycle. Ideally, each cycle results in the formation of one epitaxial monolayer of CdS.

EXPERIMENTAL

The hardware used in the formation of deposits by ECALE depends on the application, size of deposit, and the number of cycles desired. Initial studies of new compounds were and are performed using a static thin-layer electrochemical cell (TLE), such as that shown in Figure 2 [70]. The cell has a 1.25 cm^2 electrode surface area, and contains 3.2 μL of solution. A series of H-cells, glass cells equipped with fritted side compartments for holding reference and auxiliary electrodes (Figure 2), are used to hold the different solutions. The tip of the TLE is dipped into a solution and the thin layer is filled with an aliquot by capillary action. After deposition, the resulting solution is expelled by pressurizing the cell's interior with N_2 gas, through two pin holes at the tip of the TLE. The pin holes are also used for ionic conduction.

The cell can be used to form deposits with from 1 to 10 cycles, with each cycle consisting of about 10 discrete steps. Tedium becomes an important factor after about 10 cycles. Most of the work performed with the TLE's has involved executing a given number of cycles, and then stripping the resulting deposit as a last step. Conditions can usually be found for stripping such that the coverages of the two elements can be determined independently, by integration of their respective features in the stripping voltammetry. After about 10 cycles, however, the features tend to overlap and it becomes difficult to assign the charge.

Thicker films are being formed, using a thin-layer flow-cell electrodeposition system (Figure 3). The flow-cell deposition system is computer controlled to minimize tedium. In addition, the flow-cell allows the solutions to be exchanged without loss of potential control. The flow cell was constructed such that a variety of substrates can be used, and so the substrates can be easily removed for analysis. The design of the flow-cell hardware, however, has proven to be a critical factor in controlling the structure and extent of deposits formed.

The characterization of ECALE deposits is being carried out in two basic directions: the first involves the examination of the structure and morphology of deposits as a function of cycle variables, such as: flow rates, rinse volumes, rinse potentials, deposition potentials, and solution compositions. Those studies are, generally, carried out using the flow deposition system described above. Deposits formed with from 10 to 200 cycles are examined for morphological information using scanning electron microscopy (SEM), STM, and AFM. For elemental information, electron probe micro analysis (EPMA) and energy dispersive X-ray analysis (EDAX) are used. These techniques have been calibrated by dissolution of selected samples in

HNO_3, and application of inductively coupled plasma-atomic emission spectroscopy (ICP-AES), together with a set of standards. Other characterization techniques are being adopted as the flow-cell hardware, cycle program, and film quality improve. For instance, photoluminescence is being used to characterize the optical properties and deposit quality [71-77].

The other direction characterization studies are taking is in the use of high quality single crystal substrates, together with surface sensitive probes to examine deposit structure and composition at each step in the deposition cycle and after each cycle. These studies are performed, for the most part, using an ultra high vacuum (UHV) surface analysis instrument (Figure 4). The instrument is equipped with an antechamber where clean, well ordered surfaces can be prepared and used as substrates in a standard electrochemical cell. Electrodeposits are formed in this antechamber and then transferred into the analysis chamber without exposure to air. The composition of the surface is examined using Auger spectroscopy (AES) (Figure 5) and X-ray photoelectron spectroscopy (XPS) (Figure 6). The structures of deposit surfaces are being examined using LEED (Figure 7) and STM (Figure 1). The STM studies can be performed in several environments, including: UHV, air, and in-situ (in solution). These studies provide an atomic level perspective on the formation of deposits, a necessity when studying a deposition methodology based on the formation of atomic layers of the individual elements.

ELECTROCHEMICAL ATOMIC LAYER EPITAXY

One of the problems with the formation of thin films by CVD is the homogeneity of the deposit. The flow of reactants to the surface plays a major role in determining the deposition pattern. ALE was developed in the belief that if surface area limited reactions were used to control deposition, instead of the flux of reactants, more homogeneous deposits would result. Epitaxial growth of compounds should be achieved if deposition is limited to a single atomic layer of each element each cycle, avoiding three dimensional nucleation. As stated in the introduction, surface area limited reactions in electrochemistry are frequently referred to as UPD. The formation of high quality thin-film deposits using ALE methodology, however, is not a given. There are a large number of factors that still must be considered, as they must be considered in any other deposition methodology, for instance: the substrate lattice match, the substrate temperature, side reactions, substrate cleanliness, and particle formation.

The first steps in the development of an ECALE cycle for a given compound, are to determine that the desired elements deposit at underpotential, what those potentials are, and what solutions should be used. Figure 8 describes the basic potentials used in the ECALE formation of CdTe on a Au electrode. Au electrodes have been used extensively as substrates in the work described here, as Au is an excellent electrode material; as it is stable to both oxidation and reduction, and it has a surface that is easily prepared.

At present, there does not appear to be a simple way to use Reductive UPD to form the atomic layers of both elements in a cycle, for compound film over one monolayer in thickness. Figure 8 indicates that Reductive Te UPD can be performed at -0.2V (vs Ag/AgCl) from a pH 9, borate buffered $HTeO^{+}_{2}$ solution. The strategy would then be to remove the excess $HTeO^{+}_{2}$ solution, and replace it with a Cd^{+2} solution at -0.6 V, preceded by rinses with corresponding blank solutions. Reductive UPD of the Cd on the initial Te atomic layer results in formation of a CdTe monolayer (Figure 12) [16, 78].

Problems arise, however, if a second layer is to be formed by the same procedure, Reductive Te UPD at -0.2 V, as the Cd strips from the first CdTe monolayer. The present solution to this problem has been to work with the equilibrium described as Oxidative Te UPD, (analogously to equation 2). In the case of CdTe deposition, a solution of Te^{2-} could be used to form an atomic layer of Te by oxidation at a potential significantly lower than the potential used for Cd UPD. In that way, the cycle would consist of forming atomic layers of Te using a Te^{2-} solution at -1.2 V, and atomic layers of Cd using a Cd^{+2} solution at -0.6 V. The CdTe deposited would remain stable at potentials in between, facilitating film growth. The major problem with this scenario, is that Te^{2-} solutions are very unstable, relative to S^{2-} solutions, and almost impossible to work with. The analogous formation of CdS is amenable to the direct use of S^{2-} solutions, as depicted in the introduction (equation 2).

CdTe can be formed using the equilibrium between Te and Te^{2-}, although in a somewhat indirect manner. First, two or three monolayers of Te are formed on top of the Cd atomic layer from a $HTeO_2^{+}$ solution at -0.8 V. The $HTeO_2^{+}$ solution is then removed, replaced by a corresponding blank, and the potential is shifted to -1.2 V where the bulk Te is converted to Te^{2-}. The product Te^{2-} ions are then flushed away, leaving only an atomic layer of Te, bonded to the

Cd covered surface. Te and Se atomic layers have been formed in an analogous manner in ECALE cycles for a number of different compounds.

The general requirements of an ECALE cycle appear to be that an atomic layer of one element is deposited using Reductive UPD while an atomic layer of another is deposited using some form of Oxidative UPD. The elements most amenable to Oxidative UPD and compound formation are S, Se, Te, As, and Sb. The II-VI compounds have been studied the most extensively. However, more work is presently being directed towards the formation of III-V compounds such as GaAs and InSb. The ease of oxidation of Al, Ga and In, however, are problematic. The IV-VI compound PbTe is presently being studied as well. Table 1 lists the compounds investigated, thus far.

The ECALE cycle for CdTe has served as a test system. A TLE was used to perform initial studies concerned with identification of the substrates [79], potentials, and solutions [69] that should be used. Those studies were the first demonstration of the workability of the ECALE method, however only coulometric data was obtained. The experiments consisted of performing a given number of cycles, and then stripping off the deposit. The Cd and Te were quantified separately from the stripping coulometry, and the information used to determine how consistent the coverage per cycle was, as well as the stoichiometry of the deposits.

The question of whether epitaxy is really occurring in ECALE is being investigated in a series of atomic level studies of the relevant surface chemistry as well as by studies of thin-films grown using the automated flow-cell deposition system. The thin-films grown with the flow-cell can be examined using conventional structure and composition characterization techniques.

The atomic level investigations began with studies of the UPD of Te on the low index planes of Au [15]. Table 2 lists the coverages and structures observed. The electrode used consisted of a single crystal for which three faces had been oriented, cut and polished, each to a different low index plane. The three faces were all parallel to a common axis, so that after a deposition, the three faces could each be investigated sequentially, by simply rotating the crystal about this axis. Te UPD resulted in the formation of ordered Te adlattices on each of the three low index planes. Coverages were obtained from three sources: coulometry, AES, and STM. Structural information was obtained from the coverages, LEED, and STM. Deposition on Au(100) will be discussed below, as an example.

Three different Te structures were observed, corresponding to different Te coverages on Au(100). Two structures were formed at different reductive underpotentials, while a third structure was formed at potentials corresponding to bulk Te deposition. Oxidative UPD of Te was performed, as well. The first Reductive UPD structure was formed at 0.3V, and consisted of a 1/4 coverage (2X2) structure (Figure 9). This structure could be considered epitaxial, in that it was commensurate however the Te coverage was only 1/4 relative to the number of surface Au atoms. The other two structures were commensurate as well, but again they did not correspond to unit coverage. Deposition into the second UPD feature at 0.6 V (Figure 9), results in the LEED pattern shown in Figure 7 and the STM image shown in Figure 1. The LEED pattern corresponds to a (2X/10) unit-cell and a Te coverage of 1/3. The structure is very different than the simple (2X2) formed after the first peak, as the Te atoms appear to be dimerizing or forming chains on the surface. The bulk structure of Te, as mentioned in the introduction, consists of chains of atoms, and this (2X/10) structure appears analogous [44], as if the chains have been bonded to the surface with a 40% expansion in the Te-Te bond distance. This same (2X/10) structure is formed by Oxidative UPD. Bulk Te deposition appears to begin with the formation of a 2/3 coverage adlattice, with a (/2X/5) unit-cell (Figure 10). The same LEED pattern persists as bulk Te deposits are formed [15].

Subsequent Reductive Cd UPD on any one of the three Te structures described above, resulted in formation of a CdTe structure with a (/2X/2)R45° unit cell. That is, the structure and coverage of the initially deposited Te layer did not dictate the resulting CdTe structure. The clarity of the LEED patterns, however, were a function of the initial Te coverage. A proposed structure is shown in Figure 11. The structure is consistent with the observed unit-cell, identified with LEED, the coverages of both Te and Cd, and with STM images such as that shown in Figure 12 [17, 78]. The structure consists of a 1/2 monolayer of both Te and Cd. The Te atoms have been drawn in four fold sites in the Au(100) substrate, while the Cd atoms have been drawn in two fold sites in the Te atomic layer (Figure 12). The structure proposed is essentially a (100) plane from the bulk structure for CdTe (Zinc Blende), superimposed on a Au(100) surface with a 10% contraction. Similar well-ordered CdTe adlattice structures formed on the other two low index planes of Au [17, 78].

The question could be raised: what does epitaxy of a compound on an elemental substrate mean? It appears that, avoiding the strictest definition, epitaxial deposition has occurred in the

formation of the CdTe monolayers, described above. The 10% lattice mismatch, however, essentially guarantees that defects will form in the deposits as more cycles are performed and strain builds. Significant degradation in the LEED patterns was observed after a second ECALE cycle, for instance. In addition, there are inherent problems with trying to epitaxially grow a compound on an elemental substrate, as phase boundaries occur at step edges [80-83].

The next questions concern the use of lattice matched and/or compound substrates. InSb is an obvious choice for the formation of CdTe deposits as it is a compound with essentially the same lattice constant as CdTe. Au has been used extensively as a substrate in studies of ECALE because it is a relatively well understood electrode material. InSb, on the other hand, is unknown as an electrode material. The surface chemistry of InSb in aqueous solutions has just begun to be studied, and those studies are necessary precursors to the use of InSb as a substrate in ECALE deposition. Problems being addressed in those studies involve identification of the conditions under which a stoichiometric InSb surface can be formed reproducibly in solution. In and Sb dissolve at different rates, and at different potentials. It is hoped that bulk Sb can be reduced off, allowing the development of a preparation methodology similar to that previously developed for CdTe [84]. With CdTe, an oxidative etch was first used, resulting in the formation of a Te rich surface, the Cd being preferentially etched. The substrate was then negatively polarized, in order to remove the excess Te by reduction of Te^{2-}. The net result was a well-ordered and stoichiometric CdTe surface [84].

One of the important questions concerning ECALE is not whether a strictly epitaxial deposit of CdTe can be grown on a Au electrode, but whether, given a well ordered lattice matched substrate (CdTe or InSb for example), layer by layer growth occurs, and does the crystal grow only in the vertical direction? Structural determination at the scale of a few monolayers, however, is still difficult, especially when the reaction media is an aqueous solution.

Thicker films are presently being formed using the automated flow-cell deposition system described in the experimental section (Figure 3). SEM images of four deposits are shown in Figure 13. A micrograph of one of the first deposits formed with the flow-cell, using 50 cycles, is shown in Figure 13a. The texture of the deposit resembles what might be expected

if small particles formed in the solution agglomerated on the surface. Subsequent studies have indicated that antidisproportionation of Te^{2-} and $HTeO_2^+$ to form Te nuclei,

{3} $2Te^{2-} + HTeO_2^+ + 3H^+ \longrightarrow 3Te + 2H_2O$,

was probably responsible for most of the particle formed. Reaction {3} occurred in the formation of early deposits as the Te atomic layers were being formed by direct reduction from a $HTeO_2^+$ solution at -1.20V. At -1.20V, Te^{2-} was forming at the same time as the $HTeO^+_2$ was being reduced. The two ions were thus present in the cell at the same time. To prevent reaction {3}, subsequent depositions were performed as described previously. That is, a couple of monolayers of Te were first formed at -0.8V, the solution was exchanged for a corresponding blank solution, and the potential was lowered to a potential where excess Te was converted to Te^{2-}, -1.20V, eliminating mixing of the Te^{2-} and $HTeO^+_2$ ions (Figure 13b). Comparison of Figures 13a and 13b reveals that this relatively simple change in the ECALE cycle program, resulted in a large improvement in deposit quality.

Some particles are still evident in the 50 cycle deposit shown in Figure 13b, however. Films grown with 100 cycles, using the same program start to show the same kind of morphology as depicted in Figure 13a. Attempts to optimize the flow cell hardware, have shown the deposit morphology to be a relatively sensitive function of it. Problems with the hardware appear to have led to accidental mixing of the reactant species. That is, the particles in Figure 13b appears to result from accidental mixing of Cd^{+2} and Te^{2-} ions, leading to homogeneous precipitation and accumulation of the resulting particles on the surface. Improvements in the pumping, piping, valving and face-plate design have greatly improved the quality of the deposits, minimizing the mixing and thus the precipitation (Figure 13c and 13d). The only features visible in Figure 13c are attributable to the Au foil substrate, not to the 50 cycle deposit. After 150 cycles, however, features due to the deposit are clearly visible (Figure 13d). The morphology of the deposits in Figure 13d is distinctly different from that present in Figure 13a and 13b. Instead of a deposit which looks like it was formed by the agglomeration of still smaller particles, the surface looks to be covered with round buttons. Figure 14 is an image taken with an AFM of the same surface.

The term epitaxy definitely appears out of place in connection with the deposits shown in Figures 13a and 13b. However, it is quite possible that the structures shown in Figures 13d and 14 are the result of layer by layer growth on a less than ideal substrate. There are a number of possible reasons for the non-ideal morphologies. For instance, the substrate used was a piece of Au foil, with the extreme number of surface defects that that entails. There is the 10% CdTe lattice mismatch with Au. There is the phase shift problem [80-83]. It is clear, also, that the hardware has not yet been completely optimized. A small number of particles may be acting as nucleation sites on the surface. Furthermore, very little work has been done to optimize the steps in the deposition cycle. Until the particles (Figures 13a and 13b) were minimized, there was no reason to try and optimize steps in the deposition cycle itself. Present studies are being directed towards investigations of the individual steps.

Over all, the use of ECALE to epitaxially electrodeposit compounds looks promising. The hardware is improving, work on better substrates is progressing, steps in the cycle are being optimized, and a fundamental understanding of the surface chemistry is being developed. ECALE is an electrodeposition methodology that should provide for vastly increased control over the deposition process. As an example, the graph in Figure 15 shows the changes in coverage and stoichiometry for deposits made with 50 cycles, as a function of the potential used to deposit the Cd atomic layers. The central plateau region (Figure 15) is an indication that there is little variation in the stoichiometry or coverage over a significant potential range, as would be expected for a process controlled by the surface area of the deposit. At the most negative potentials, however, the coverage starts to go up, as the potential range for Cd UPD is exceeded, and bulk Cd begins to form. At the most positive potentials, the coverages for both Cd and Te drop, as no Cd appears to be depositing at all.

ACKNOWLEDGMENTS

Acknowledgment is made to the Department of the Navy, Office of the Chief of Naval Research, under Grant No. N00014-91-J-1919. Acknowledgment is also made to the National Science Foundation for partial support of this work under Grant No. DMR-9017431.

REFERENCES

1. K.R. Lawless, *J. Vac. Sci. Technol.*, 2, 24 (1965).

2. K.R. Lawless in Physics of Thin Films, vol. 4 of Advances in Research and Development, G. Haas and R.E. Thun, eds., Academic Press, 1967.

3. J.G. Wright in Epitaxial Growth, J.W. Matthews, editor, Academic Press, p. 82, 1975.

4. D.M. Kolb, In Advances in Electrochemistry and Electrochemical Engineering, H. Gerischer, C.W. Tobias Eds., Vol. 11, Wiley, New York, 1978, p. 125.

5. K. Jutter and W.J. Lorenz, Z. Phys. Chem. N.F., 122 (1980) 163.

6. R.R. Adzic, In Advances in Electrochemistry and Electrochemical Engineering, H. Gerischer, C.W. Tobias, Eds., Vol. 13, Wiley-Interscience: New York, 1984, p.159-260.

7. J.Clavilier, D. Armand, and B.L. Wu, J. Electroanal. Chem., 135 159 (1982).

8. J. Clavilier and D. Armand, *J. Electroanal. Chem.*, 199, 187 (1986).

9. D.A. Stern, H. Baltruschat, M. Martinez, J.L. Stickney, D. Song, S.K. Lewis, D.G. Frank and A.T. Hubbard, *J. Electroanal. Chem.*, 217, 101 (1987).

10. G.N. Salaita, D.A. Stern, F. Lu, H. Baltruschat, B.C. Schardt, J.L. Stickney, M.P. Soriaga, D.G. Frank and A.T. Hubbard, *Langmuir*, 2, 828 (1986).

11. I. Villegas, D.W. Suggs, J.L. Stickney, B.G. Bravo and M.P. Soriaga, *J. Phys. Chem.*, **95**, 5245 (1991).

12. I.C. Hamilton and R. Woods, *J. Appl. Electrochem.*, **13**, 783 (1983).

12. J.M.M. Droog, C.A. Alderliesten, P.T. Alderliesten and G.A. Bootsma, *J. Electroanal. Chem.*, **111**. 61 (1980).

13. L.P. Colletti, D. Teklay and J.L. Stickney, *J. Electroanal. Chem.*, in press.

14. Authors unpublished results.

15. D.W. Suggs and J.L. Stickney, *J. Phys. Chem.*, **95**, 1310 (1991).

16. D.W. Suggs and J.L. Stickney, *Surface Sci.*, **290**, 375 (1993).

17. I. Villegas and J.L. Stickney, *J. Electrochem. Soc.*, **139**, 686 (1992).

18. J.L. Stickney, S.D. Rosasco, D. Song, M.P. Soriaga and A.T. Hubbard, *Surface Sci.*, 130, 326 (1983).

19. M.P. Green, M. Richter, X. Xing, D. Scherson, K.J. Hanson, P.N. Ross, Jr., R. Carr and I. Lindau, *Jrl. of Microscopy*, **152**, 823 (1988).

20. M.P. Green, K.J. Hanson, D.A. Scherson, X. Xing, M. Richter, P.N. Ross, Jr., R. Carr and I. Lindau, *J. of Phys. Chem.*, **93**, 2181 (1989).

21. O.M. Magnussen, J. Hotlos, R.J. Nichols, D.M. Kolb, and R.J. Behm, *Phys. Rev. Lett.*, **64**, 2929 (1990).

22. O.M. Magnussen, J. Hotlos, G. Beitel, D.M. Kolb, and R.J. Behm, *J. Vac. Sci. Technol. B*, 9, 969 (1991).

23. S. Manne, P.K. Hansma, J. Massie, V.B. Elings, A.A. Gewirth, *Science*, 251, 183 (1991).

24. S. Manne, J. Massie, V.B. Elings, P.K. Hansma, A.A. Gewirth, *J. Vac. Sci. Technol. B*, 9, 950 (1991).

25. C. Chen, S.M. Vesecky, and A.A. Gewirth, *J. Am. Chem. Soc.*, 114, 451 (1992).

26. M.G. Samant, M.F. Toney, G.L. Borges, L. Blum and O.R. Melroy, *J. Phys. Chem.*, 92, 220 (1988).

27. O.R. Melroy, M.F. Toney, G.L. Borges, M.G. Samant, J.B. Kortright, P.N. Ross, and L. Blum, *Phys. Rev. B*, 38, 10962 (1988).

28. M.F. Toney and J. McBreen, *Interface*, 2, 22 (1993).

29. J. Wang, G.M. Watson, and B.M. Ocko, *Physica A*, 200, 679 (1993).

30. B.M. Ocko, G.M. Watson, and J. Wang, *J. Phys. Chem.*, 98, 897 (1994)

31. K. Sashikata, H. Honbo, N. Furuya and K. Itaya, *Bull. Chem. Soc. Jpn.* 63, 3317 (1990).

32. X. Gao and M.J. Weaver, *J. Am. Chem. Soc.*, 114, 8544 (1992).

33. W. Haiss, J.K. Sass, X. Gao and M.J. Weaver, *Surf. Sci. Lett.*, *274*, L593 (1992).

34. R.L. McCarley and A.J. Bard, *J. Phys. Chem.*, 95, 9618 (1991).

35. N.J. Tao and S.M. Lindsay, *J. Phys. Chem.*, 96, 5213 (1992).

36. T.E. Felter and A.T. Hubbard, *J. Electroanal. Chem.*, **100**, 473 (1979).

37. G.A. Garwood and A.T. Hubbard, *Surf. Sci.*, **92**, 617 (1980).

38. A. Wieckowski, S.D. Rosasco, B.C. Schardt, J.L. Stickney and A.T. Hubbard, *Inorg. Chem.*, **23**, 565 (1984).

39. A. Wieckowski, S.D. Rosasco, J.L. Stickney and A.T. Hubbard, *Surface Sci.*, **146**, 115 (1984).

40. Discussion with Andrew A. Gewirth.

41. D.F. Ogletree, R.Q. Hwang, D.M. Zeglinski, A. Lopez Vazquez-de-Parga, G.A. Somorjai and M. Salmeron, *J. Vac. Sci. Technol. B*, **9**, 886 (1991).

42. G.A. Somorjai and M. Salmeron in ACS Symposium Series, Vol. 485, p. 103-111 (1992).

43. J.C. Dunphy, P. Sautet, D.F. Ogletree and M.B. Salmeron, *J. Vac. Sci. Technol. A*, **11**, 2145 (1993).

44. N.N. Greenwood and A. Earnshaw, *Chemistry of the Elements*, Peragmon Press, 1984.

45. J.H. van der Merwe, *CRC Crit. Rev. in Solid State and Mat. Sci.*, **209** (1978).

46. S. Sharan, J. Narayan and K. Jagannadham, *Mat. Res. Soc. Symp. Proc.*, Vol. 102.

47. C. Fontaine, J.P. Gailliard, S. Magli, A. Million, and J. Piaguet, *Appl. Phys. Lett.*, **50**, 903 (1987).

48. J.L. Stickney and M.L. Norton in "*Electroanalytical Chemistry,*" ed. A.J. Bard, Marcel Dekker, New York, in preparation.

49. B.W. Gregory and J.L. Stickney, *J. Electroanal. Chem.*, **300**, 543 (1991).

50. G.F. Fulop and R.M. Taylor, *Ann Rev. Mater. Sci.*, **15**, 15 (1985).

51. H. Von Gobrecht, H.-D. Liess and A. Tausend, *Ber. Bunsenges. Phys. Chem.*, **67**, 930 (1963).

52. A.J. Panson, *Inorg. Chem.*, **3**, 940 (1964).

53. B. Miller and A. Heller, *Nature*, **262**, 680 (1976).

54. J. Vedel, M. Soubeyrand and E. Castel, *J. Electrochem. Soc.*, **124**, 177 (1977).

55. L.M. Peter, *Electrochimica Acta*, **23**, 165 (1977).

56. B. Miller, S. Menezes and A. Heller, *J. Electroanal. Chem.*, **94**, 85 (1978).

57. J.F. McCann and M.S. Kazacos, *J. Electroanal. Chem.*, **119**, 409 (1981).

58. V.I. Birss and L.E. Kee, *J. Electrochem. Soc.*, **133**, 2097 (1986).

59. D. Ham, Y. Son, K.K. Mishra and K. Rajeshwar, *J. Electroanal. Chem.*, **310**, 417 (1991).

60. C. Shannon and B. Pettinger, *J. Electroanal. Chem.*, submitted.

61. W.J. Danaher and L.E. Lyons, *Nature*, **271**, 139 (1978).

62. M.P.R. Panicker, M. Knaster, and F.A. Kroger, *J. Electrochem. Soc.*, **125**, 566 (1977).

63. Y. Golan, L. Margulis, I. Rubinstein and G. Hodes, *Langmuir*, **8**, 749 (1992).

64. M.L. Norton, *Materials Research Bulletin*, **24**, 1391 (1989).

65. J.A. Switzer, M.J. Shane, and R.J. Phillips, *Science*, **247**, 444 (1990).

66. T. Suntola and J. Antson, U.S. Patent 4,058,430 (1977).

67. S. Bedair, "Atomic Layer Epitaxy," Elsevier, Amsterdam, 1993.

68. T.F. Kuech, P.D. Dapkus, Y. Aoyagi, "Atomic Layer Growth and Processing," Materials Research Society, Pittsburgh, 1991.

69. B.W. Gregory, D.W. Suggs and J.L. Stickney, *J. Electrochem. Soc.*, **138**, 1279 (1991).

70. A.T. Hubbard, *CRC Critical Rev. in Anal. Chem.*, 201 (1973).

71. E. Molva, K. Saminadayar, J.L. Pautrat, and E. Ligeon, *Solid State Comm.*, **48**, 955 (1983).

72. N.C. Giles-Taylor, R.N. Bicknell, D.K. Blanks, T.H. Myers, and J.F. Schetzina. *J. Vac. Sci. Technol. A*, **3**, 76 (1985).

73. J.M. Figueroa, F. Sanchez-Sinencio, J.G. Mendoza-Alvarez, O. Zelaya, C. Vazquez-Lopez, and J.S. Helman, *J. Appl. Phys.*, **60**, 452 (1986).

74. K.M. James, J.D. Flood, J.L. Merz, and C.D. Jones, *J. Appl. Phys.*, **59**, 3596 (1986).

75. J. Landa-Garcia, M. Cardenas, G.C. Puente, J.G. Mendoza-Alvarez, F. Sanchez-Sinencio, and O. Zelaya, *J. Vac. Sci. Technol. A*, **8**, 79 (1990).

76. P.M. Amirtharaj and N.K. Dhar, *J. Appl. Phys.*, **67**, 3107 (1990).

77. J. Landa-Garcia, M. Cardenas, G.C. Puente, J.G. Mendoza-Alvarez, F. Sanchez-Sinencio, and O. Zelaya, *J. Vac. Sci. Technol. A*, **8**, 79 (1990).

78. D.W. Suggs and J.L. Stickney, *Surf. Sci.*, **290**, 362 (1993).

79. B.W. Gregory, M.L. Norton and J.L. Stickney, *J. Electroanal. Chem*,. **293**, 85 (1990).

80. H. Kroemer, *Jrl. of Crys. Growth*, **81**, 193 (1987).

81. K. Morizane, *Jrl. of Crys. Growth*, **38**, 249 (1977).

82. N.-H. Cho, B.C. De Cooman, C.B. Carter, R. Fletcher and D.K. Wagner, *Appl. Phys. Lett.*, **47**, 879 (1985).

83. S. Strite, M.S. Unlu, K. Adomi, G.-B. Gao, A. Agarwal, A. Rockett, H. Morkoc, D. Li, Y. Nakamura and N. Otsuka, *J. Vac. Sci. Technol. B*, **8**, 1131 (1990).

FIGURE CAPTIONS

Figure Captions, Huang et al. *"FIGCAPS.SAM"*

Figure 1: STM micrographs of Au(100)(2X/10)-Te structure, observed after scanning to the onset of the second Te UPD feature and emersing. Height mode, V_b = -0.5 mV, i_t= 5 nA.

Figure 2: Diagram of the thin layer electrochemical cell (TLE) used to perform preliminary ECALE studies. A) TLE mounted in the H-cell and B) enlargement of the pinhole region.

Figure 3: Diagram of the automated thin layer flow deposition system, used in the formation of thicker deposits by the ECALE methodology. Pumps and valves are computer controlled and regulate the introduction of solutions to the thin-layer cell. A potentiostat is interfaced as well, and controls the deposition potentials.

Figure 4: Schematic of the ultra high vacuum-electrochemical (UHV-EC) system used to study deposit coverages and structures.

Figure 5: Auger spectra of the Au(100) surface: A) following Cd UPD, B) following 1st Te UPD, C) following Cd UPD on 1st Te UPD, and D) following Cd UPD on a 2nd Te UPD.

Figure 6: XPS spectra of Au(100) after A) ion-bombardment and annealing, B) 1st Te UPD, C) Cd UPD on 1st Te UPD, and D) deposition of Bulk Te.

Figure 7: LEED pattern showing the Au(100)(2X/10)-Te structure following emersion at the onset of the second Te UPD feature. 14.5 eV.

Figure 8: Potential diagram for ECALE of CdTe.

Figure 9: Voltammetry of Au(100) in 0.2mM TeO_2 + 10 mM H_2SO_4. v = 5 mV/sec.

Figure 10: LEED of the (/2X/5) structure, formed after the 2nd Te UPD peak. 39.1 eV.

Figure 11: Proposed Au(100)(/2X/2)R45-CdTe structure.

Figure 12: STM micrograph of Au(100)(/2X/2)-CdTe structure. Height mode, V_b= 173.9 mV, i_t= 8.4 nA

Figure 13: SEM micrographs of four deposits. The conditions are as follows: a) Te atomic layers deposited at -1.25V directly, old hardware, 50 cycles; b) bulk Te deposited at -0.8V, followed by subsequent stripping of excess Te at -1.25V, old hardware, 50 cycles; c) Same as (b) new hardware design, 50 cycles; d) same as c) but with 150 cycles.

Figure 14: AFM micrograph of CdTe deposit formed by 150 ECALE cycles, same conditions as in Figure 13d.

Figure 15: Graph of Cd and Te coverages, determined by EPMA of a series of CdTe deposits, each formed by 50 ECALE cycles. Each deposits was formed using a different Cd deposition potential. Cd = open circles and Te = crosses. Filled circles represent the concentration ratio of the two elements, as an indication of the deposit stoichiometry.

Table 1: Compounds formed with the ECALE methodology.

Table 2: Structures and coverages observed on the low-index planes of Au, after the electrodeposition of various amounts of Te.

F igure 1, Huang et al.

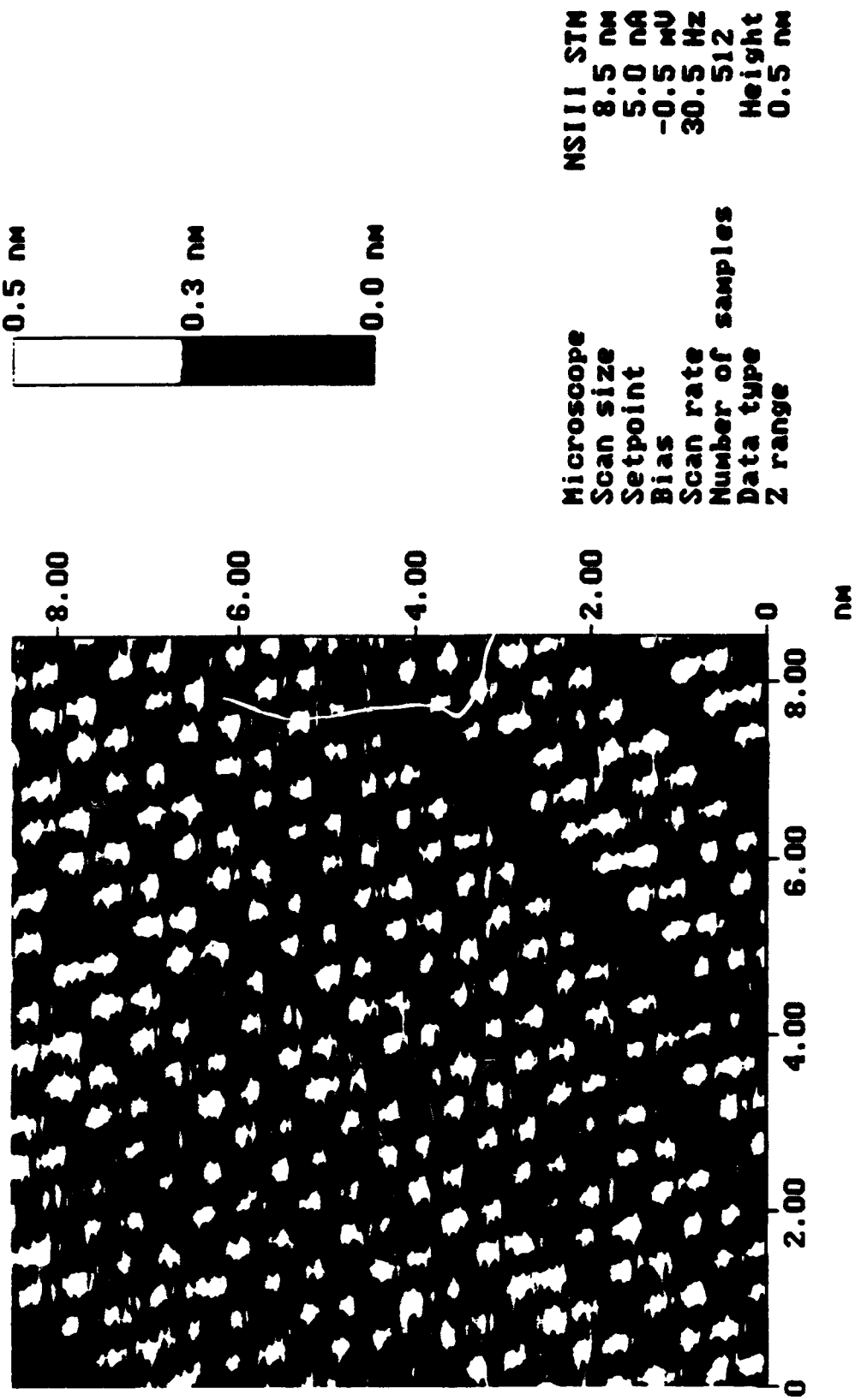

Figure 2, Huang et al.

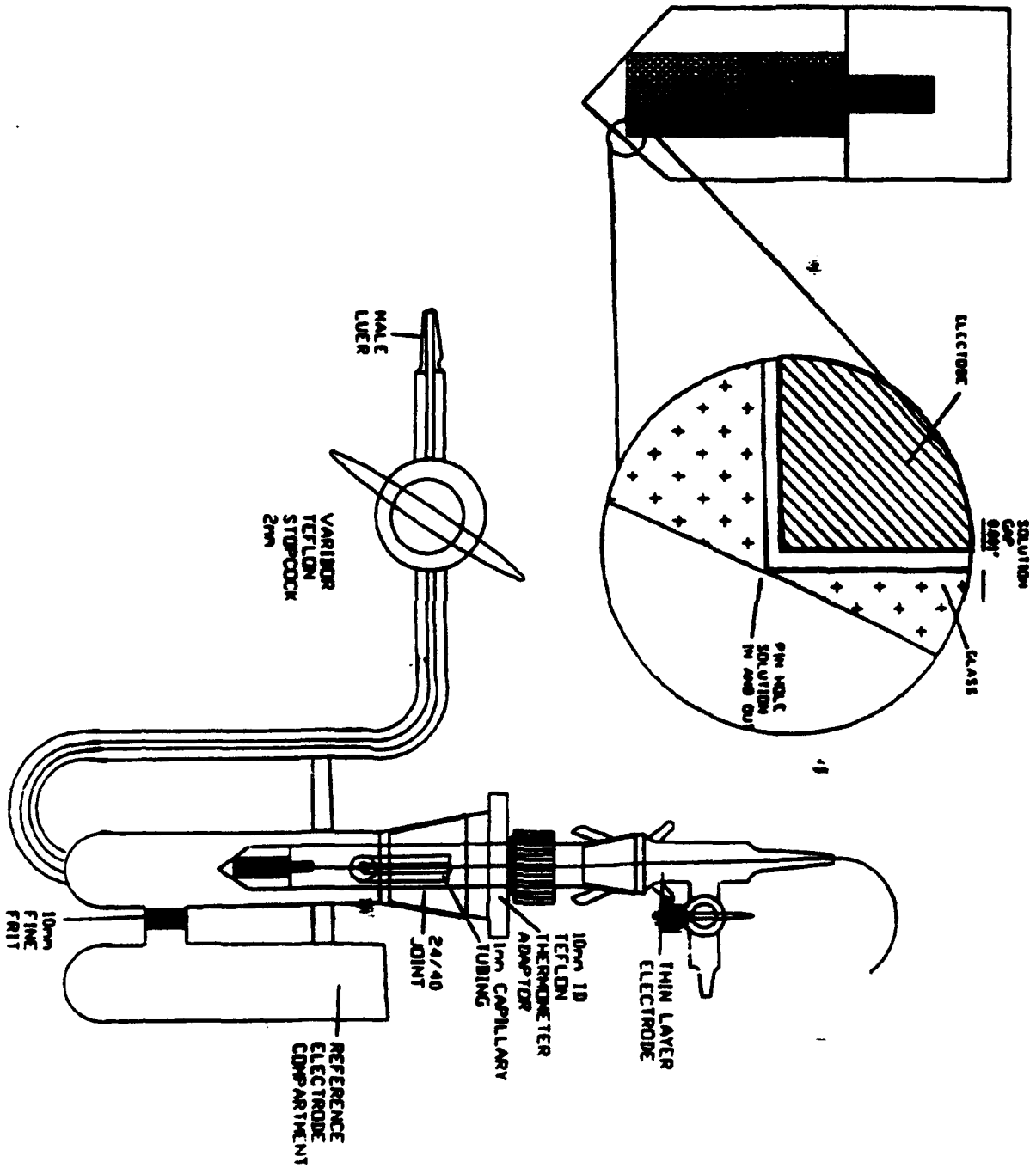

Figure 3, Huang et al.

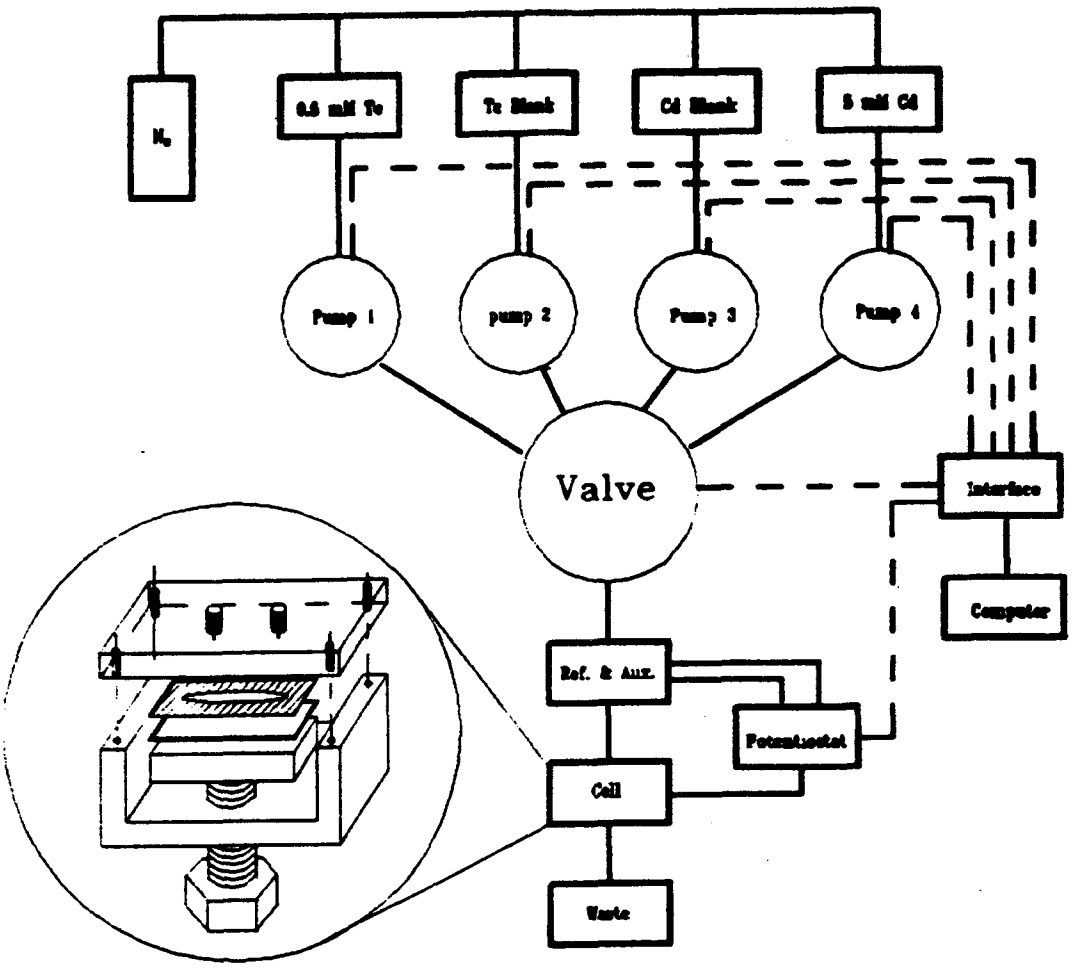

Figure 4, Huang et al.

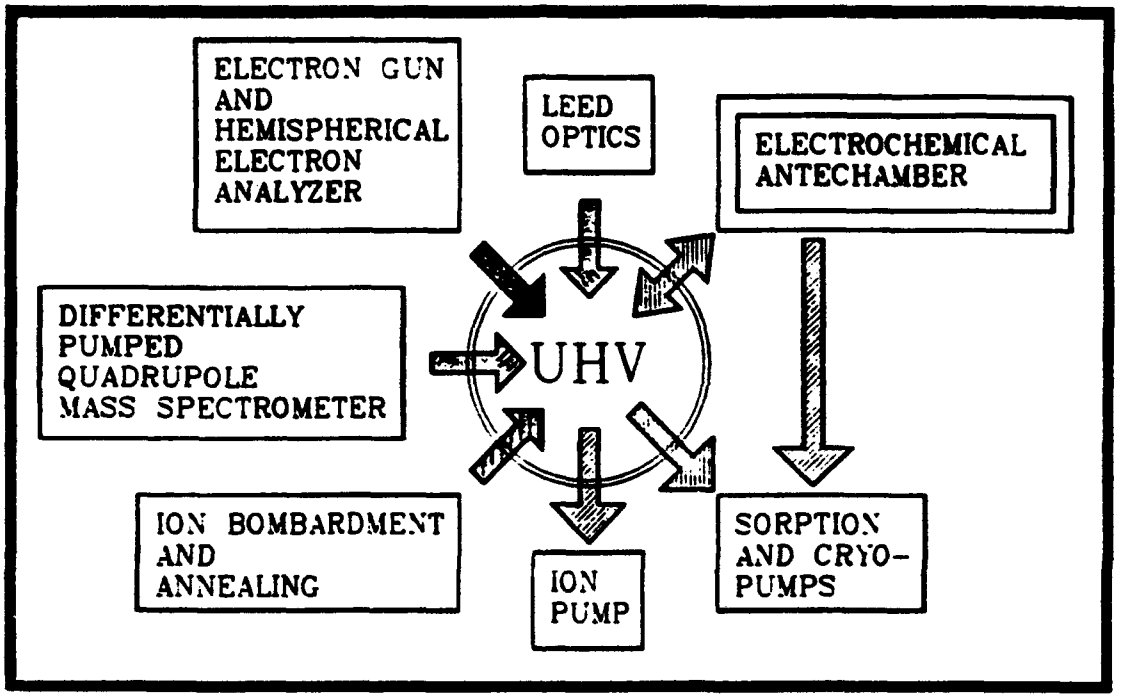

Figure 5, Huang et al.

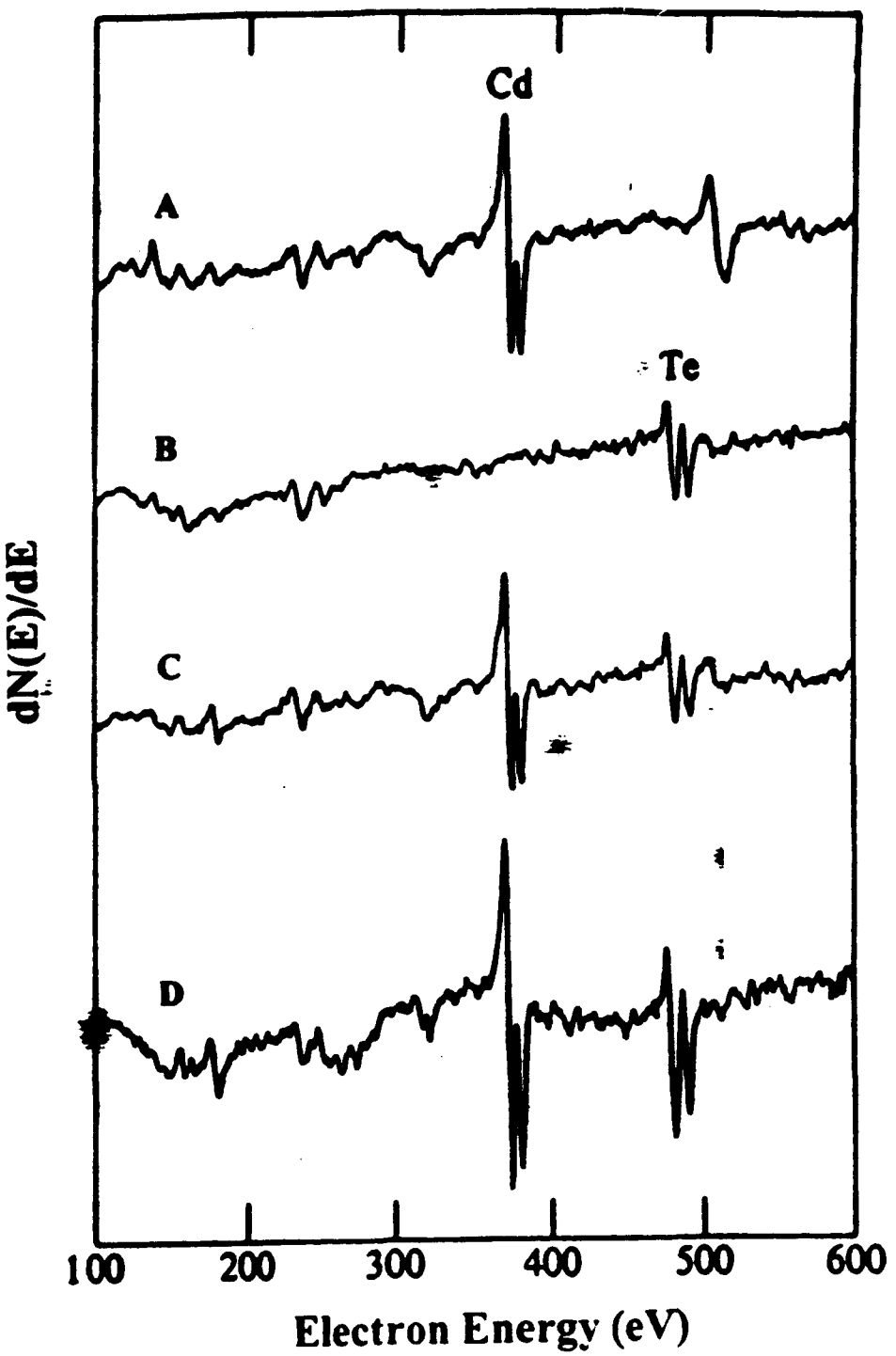

Figure 6. Huang et al

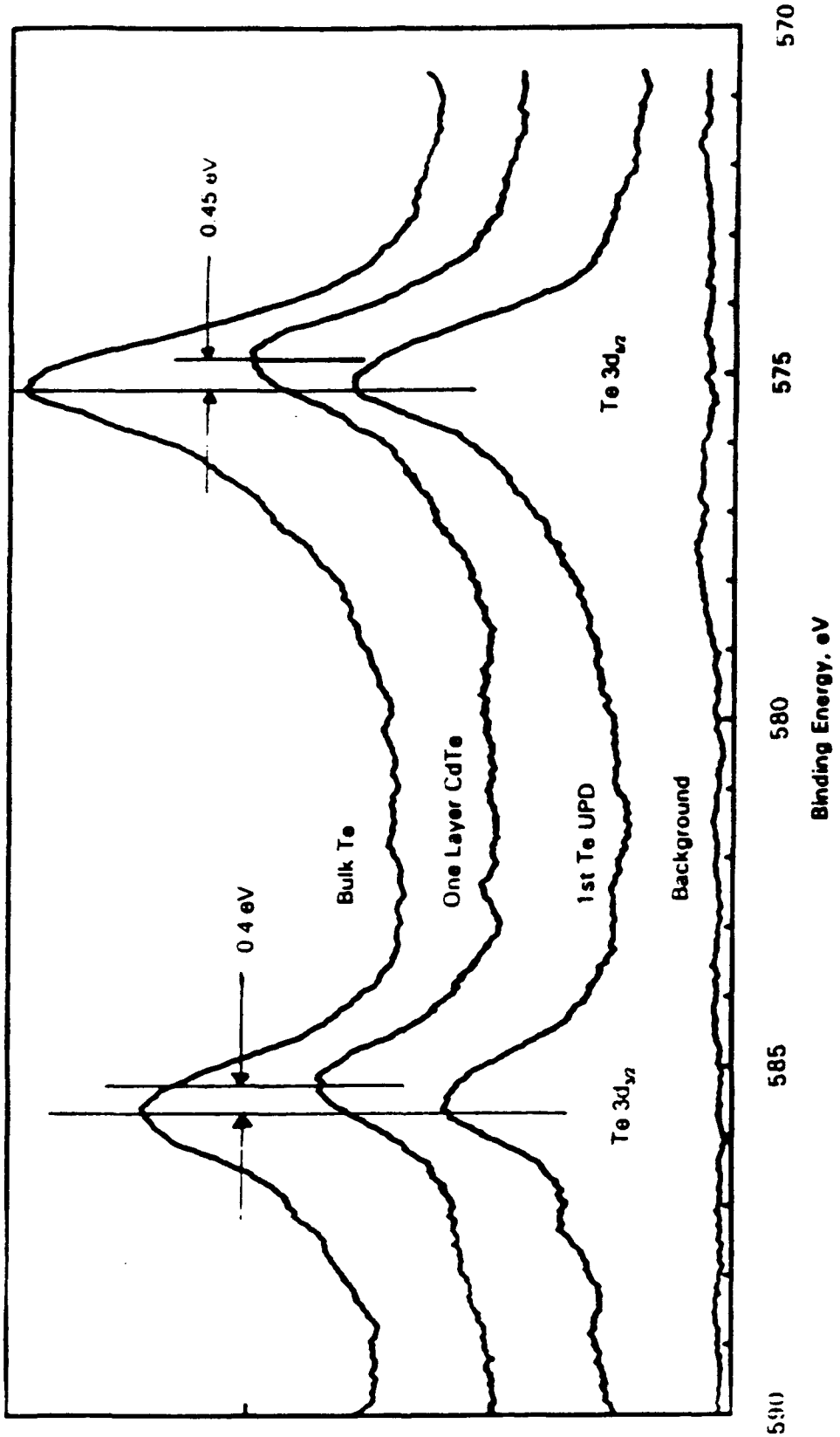

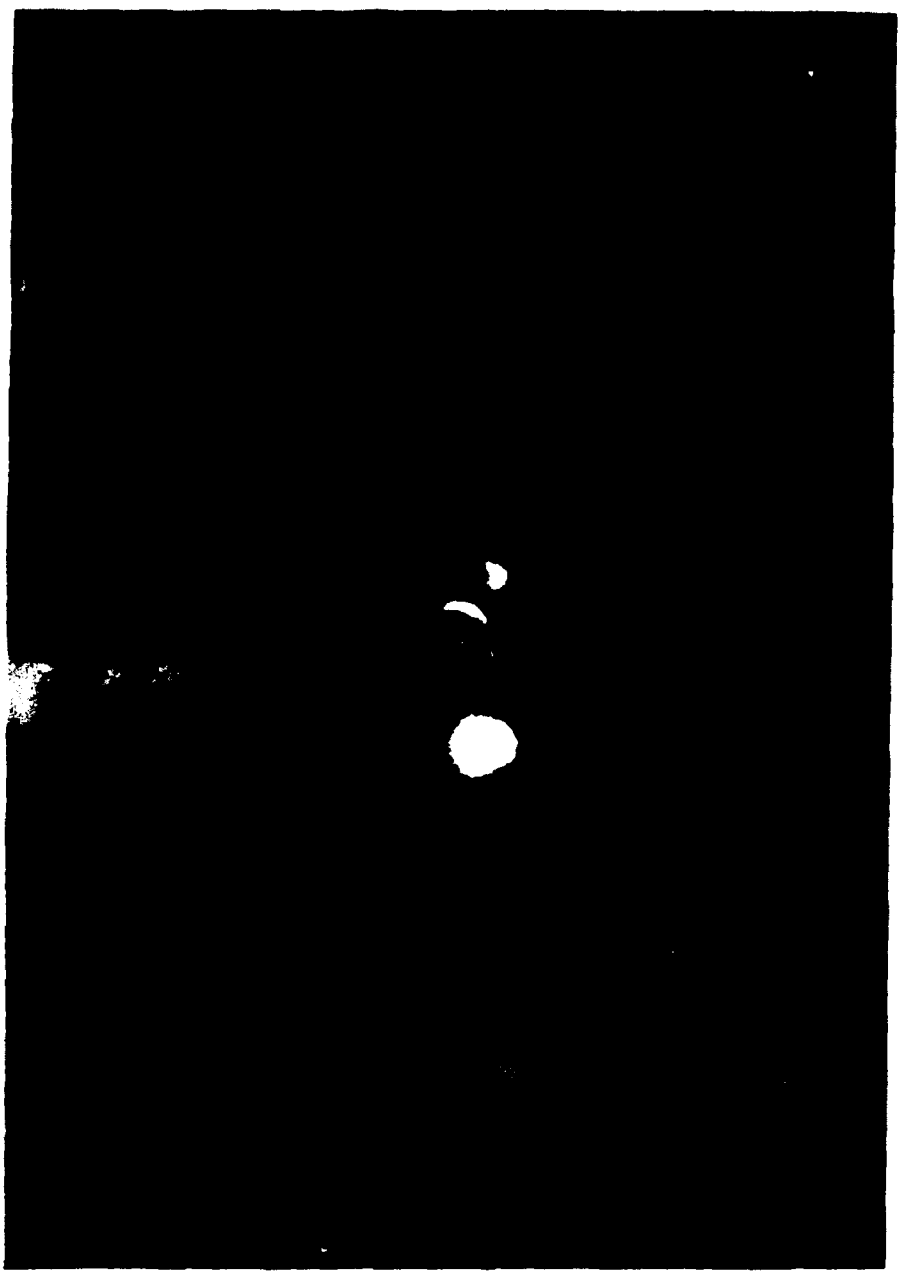

Figure 8. Huang et al.

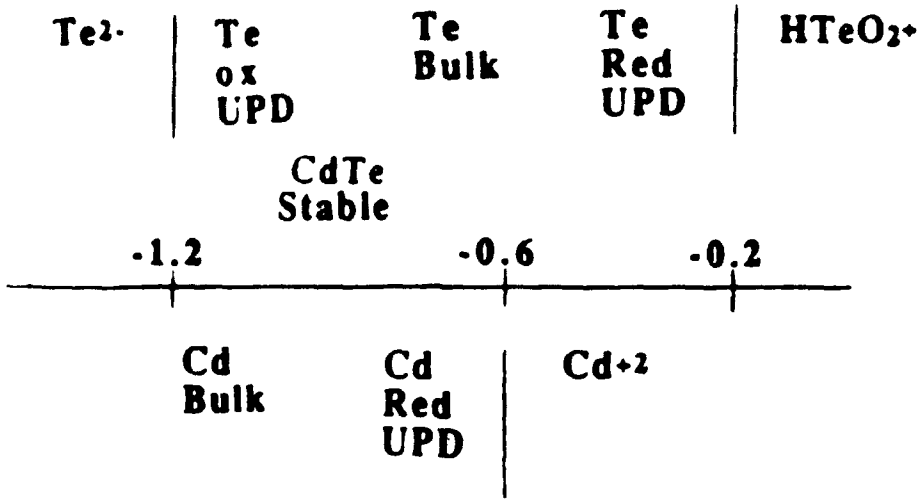

Figure 1 Huang et al

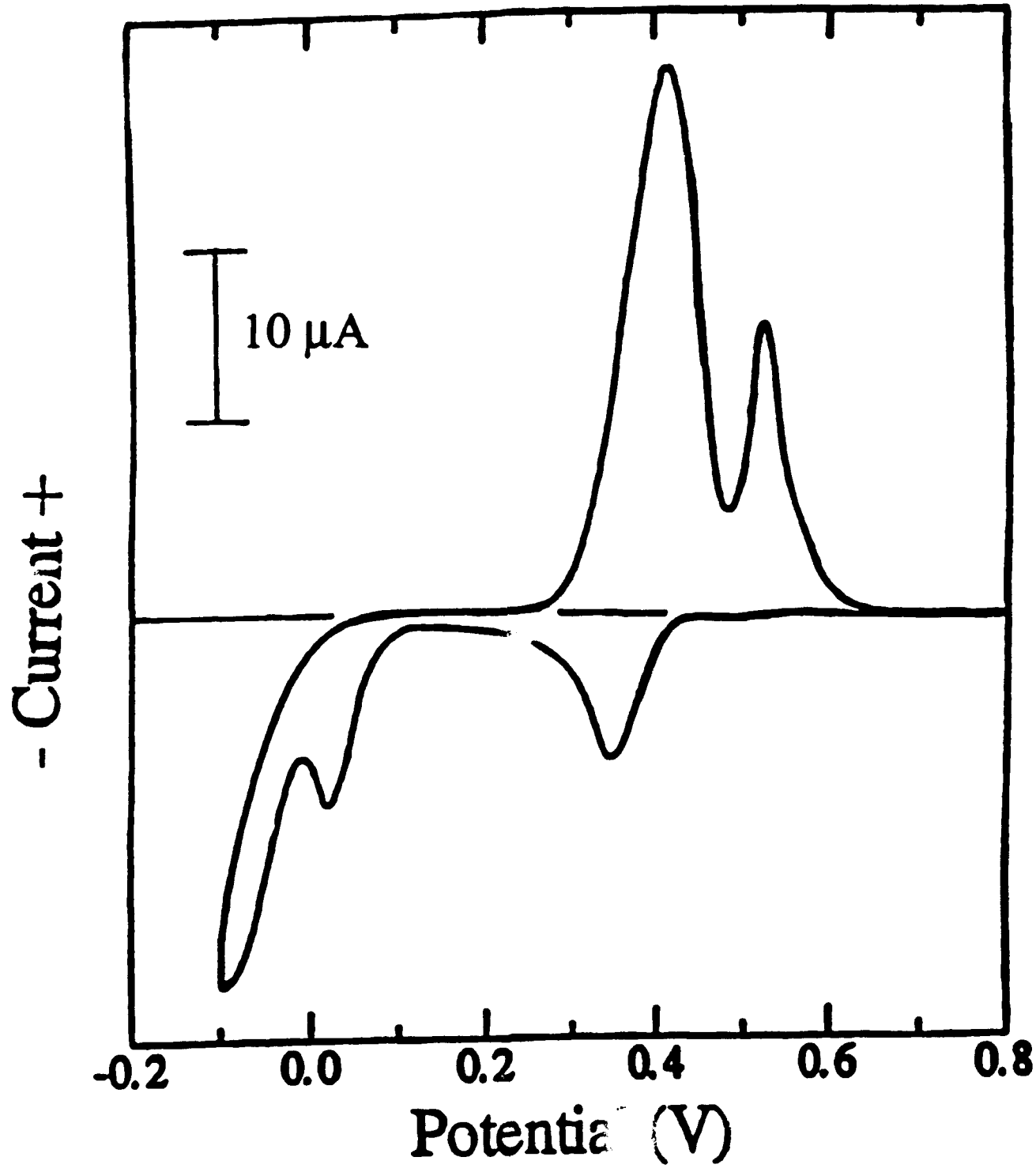

Figure 1. Hoang et al

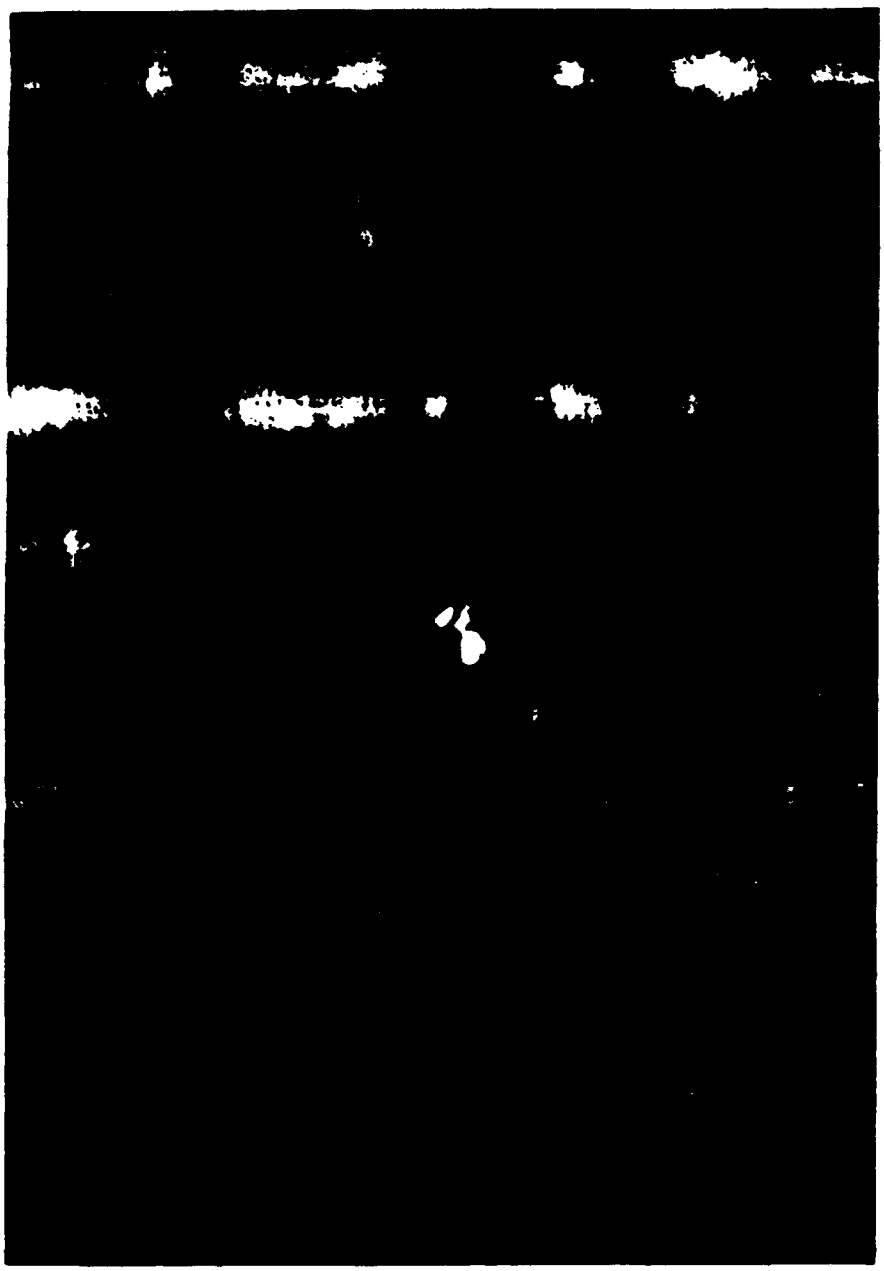

Figure 11. Huang et al.

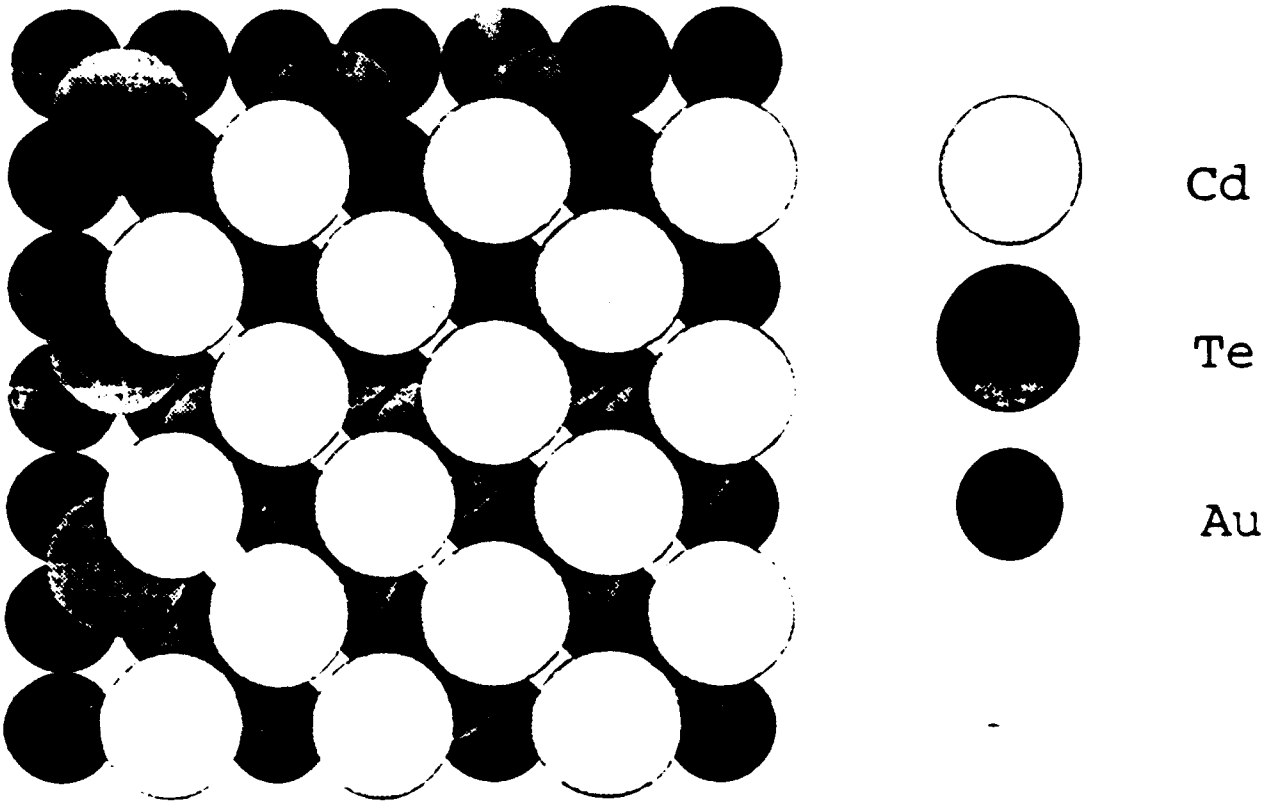

Figure 12. Huang et al.

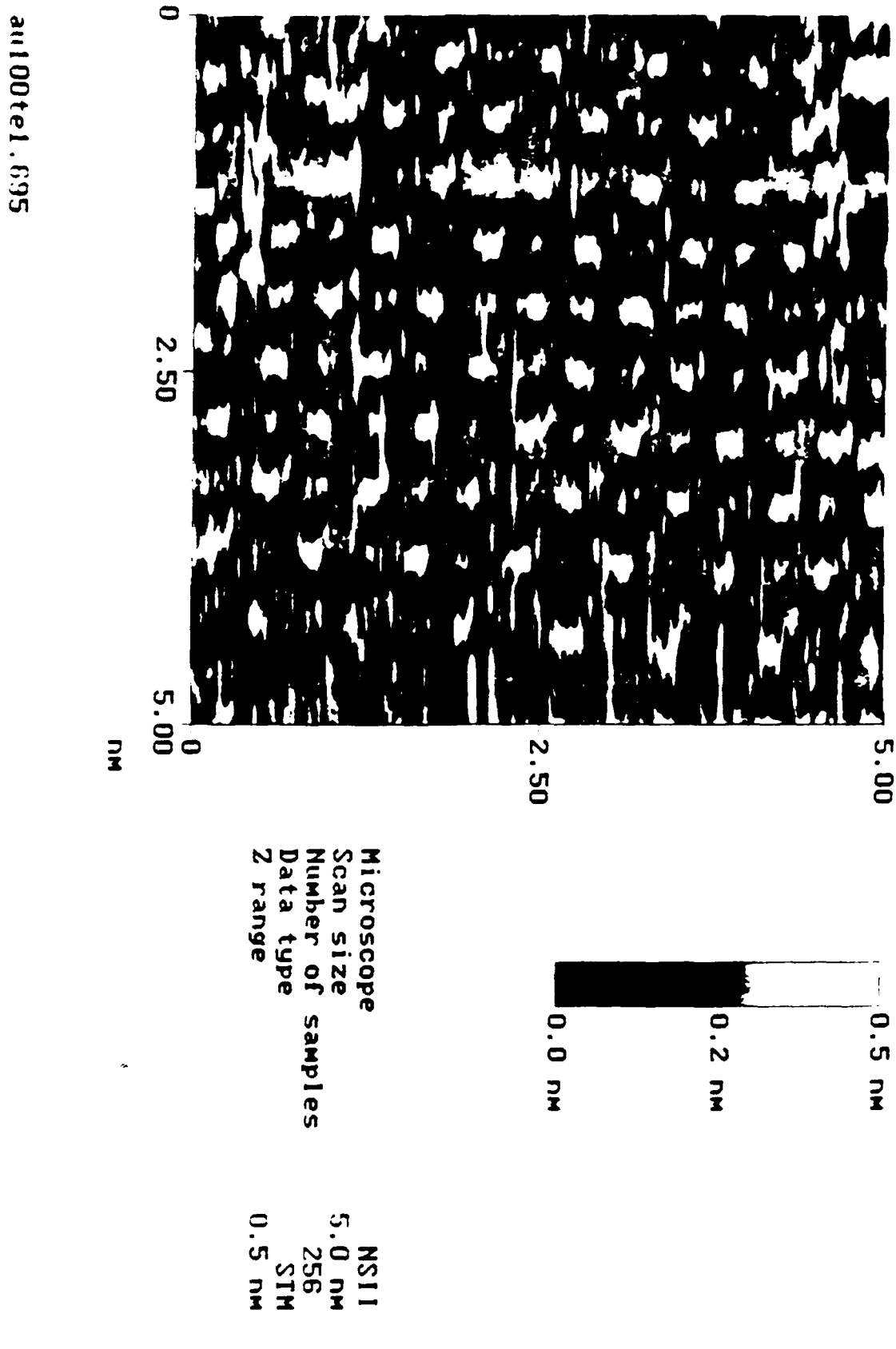

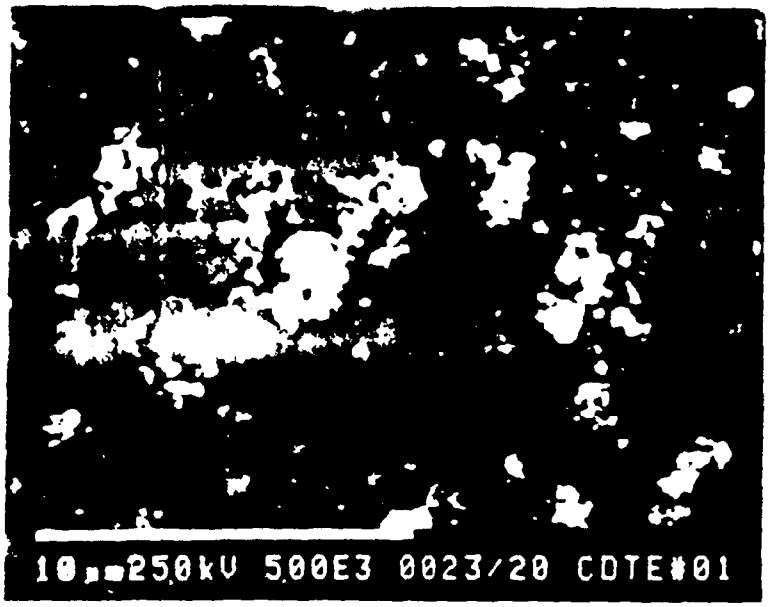
10µm250kV 500E3 0023/20 CDTE#01

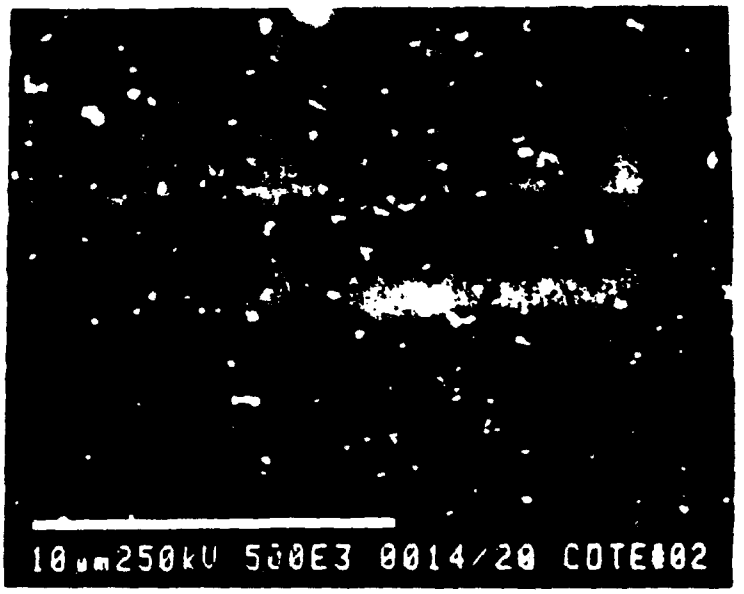
10µm250kV 500E3 0014/20 CDTE#02

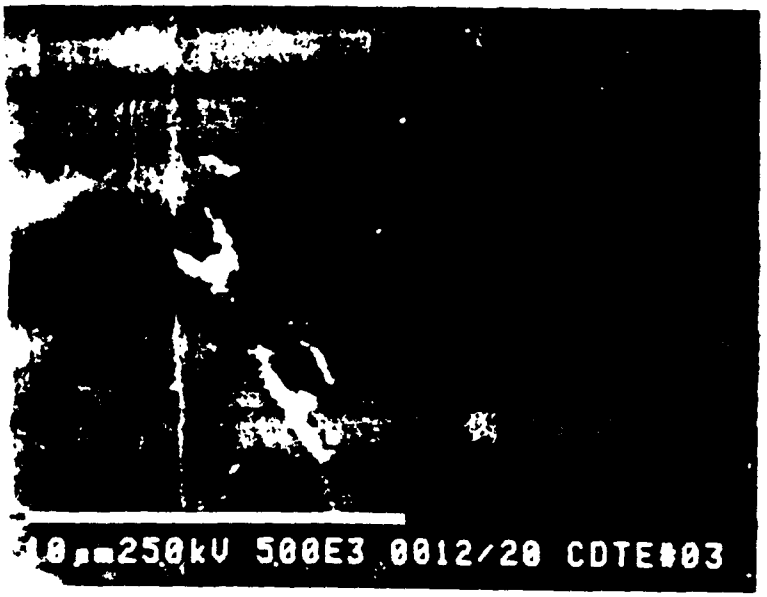
10µm250kV 500E3 0012/20 CDTE#03


10µm250kV 500E3 0016/20 CDTE#04

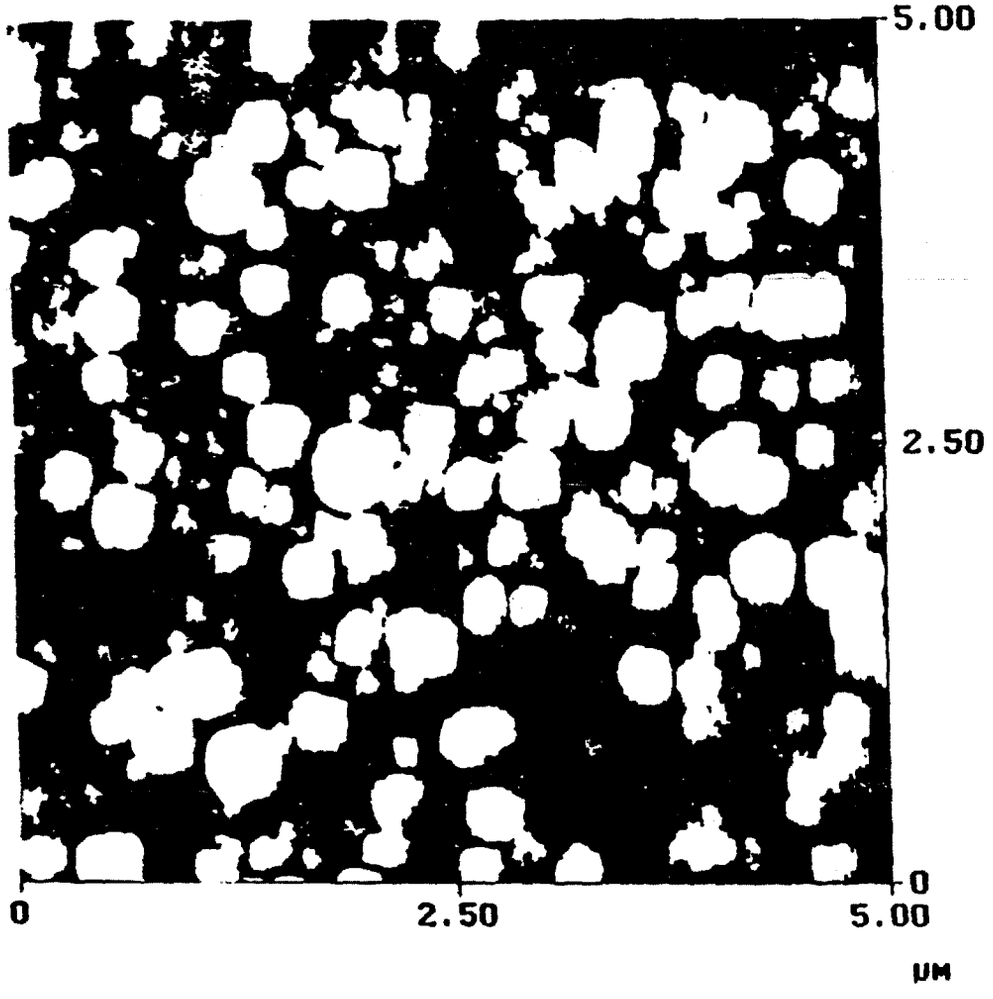

1.0 µM

0.5 µM

0.0 µM

Microsoope	NSIII AFM
Scan size	5.0 µM
Setpoint	0.0 V
Scan rate	4.1 Hz
Number of samples	512

150 ECALE-cycle CdTe with pe tic pumps
09020053.001

Figure 14. Huang et al

Figure 15. Huang et al.

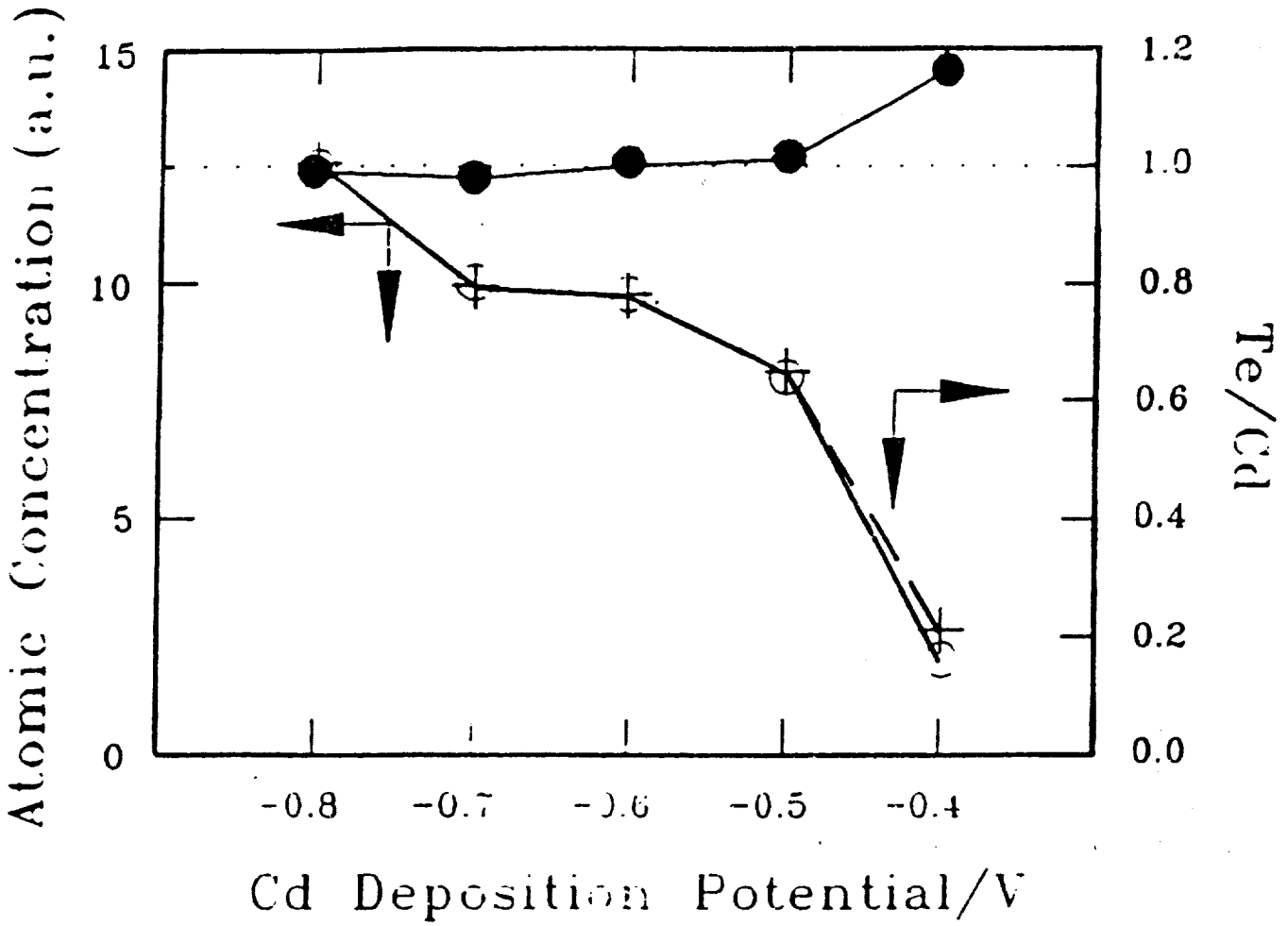

Table 1: Huang et al

Compound Semiconductor Formation By (ECALE)

II-VI	O	S	Se	Te	
Zn		YES	YES	YES	
Cd		YES	YES	YES	
Hg			YES	U	
IV-VI					
Sn		P	P	P	
Pb		P	YES	U	
III-V	**N**	**P**	**As**	**Sb**	**Bi**
Al					
Ga			YES	P	
In			P	U	
Tl			P	P	

P= Probably, but has not yet been investigated
U= Under investigation

Table 2. Huang et al.

	Feature	Potential[i] (V)	Coverage[ii]	LEED Pattern
Au(100)	First UPD	0.20	0.37	(2X2)
	Second UPD	0.00	0.90	(√2X 5)R45°
	Bulk	-0.50	3.10	(√2X 5)R45
	Oxidative UPD	-1.30	0.47	(2X/10)
Au(110)	First UPD	0.20	0.50	c(2X8)
	Second UPD	0.00	0.71	c(2X6)
	Bulk	-0.50	2.21	Diffuse (1X1)
	Oxidative UPD	1.30	0.50	c(2X8)
Au(111)	First UPD	0.20	0.48	(12X12)
	Transition	0.16	0.64	(3X3)
	Second UPD	0.00	1.09	Complex pattern
	Bulk	-0.05	3.47	ring pattern
	Oxidative UPD	1.30	0.47	(12X12)

(i) Potentials are referenced to a Ag/AgCl made with 1M NaCl
(ii) Coverages are given as x10^{15} tellurium atoms /cm2. These coverages are based on the tellurium Auger current where a conversion factor of 5.03 X 10^{13} was used.